MECHANISM OF INTERACTION BETWEEN PIOGLITAZONE HYDROCHLORIDE AND BOVINE TRANSFERRIN BY SPECTROSCOPIC AND MOLECULAR DOCKING METHODS

C. D. Wang, B. S. Liu*, G. Bian, L. H. Ma, H. C. Zhang, X. Cheng D

Key Laboratory of Analytical Science and Technology of Hebei Province,
National Chemistry Experimental Teaching Demonstration Center Hebei University,
Key Laboratory of Pharmaceutical Chemistry and Molecular Diagnosis,
Ministry of Education, Baoding, China.

Article History: Received 18.4.2018; Revised 8.12.2018; Accepted 11.12.2018

ABSTRACT

The binding of pioglitazone hydrochloride with bovine transferrin was investigated by spectroscopic and molecular docking methods under different temperature conditions (298, 310 and 318 K). The results demonstrate that the interaction between pioglitazone hydrochloride and bovine transferrin is taking place via static quenching with 1:1 binding ratio. The fluorescence data were treated by using the double logarithmic equation, and the binding constants Ka of the interaction of pioglitazone hydrochloride-bovine transferrin systems and the number of binding sites n were obtained. The thermodynamic parameters of pioglitazone hydrochloride-bovine transferrin systems under different temperatures were obtained by the thermodynamic equation. The experimental data show that the interactions between them are mainly electrostatic force interaction, which is consistent with the molecular docking results.

***KEYWORDS**: Spectrometry; molecular docking; pioglitazone hydrochloride; bovine transferrin; interaction mechanism*

1.0 INTRODUCTION

Currently, the interaction of drugs and protein has been studied widely. Binding of drugs to plasma proteins has vital implications for drug disposition and action. The effect of a drug depends on the availability of free drug in plasma. The free drug in plasma can bind to the receptor sites and exerting pharmacological action. The free concentration and pharmacologic activity of

* Corresponding e-mail: lbs@hbu.edu.cn.

the drug in vivo is closely related to its binding capacity towards transport protein (Lin et al., 2014). Moreover, the interaction of drugs with proteins may significantly affect their distribution, metabolism, excretion and toxicity in vivo. It forms the basis to re-design or modify the drug molecules, and is an important way to understand the biological effects of protein. Therefore, a comprehensive understanding of the binding characteristics of drugs to proteins at a molecular level is imperative and worthwhile.

Pioglitazone hydrochloride (PGH) (molecular structure in Figure 1) is used to treat type 2 diabetes (Zhang & Matzger, 2017). It belongs to the Biopharmaceutics Classification System (BCS) Class II because of its low solubility in water (0.047 mg/mL) (Takagi et al., 2006). Chemical hypoglycemic drugs are strictly limited in dosage, too much, there is a risk of coma or even death. Therefore, it is very important to understand the binding behavior of PGH to protein.

The transferrin (TF) family is a group of single-chain, glycosylated proteins defined by conserved residue motifs and iron-binding functions (Bai et al., 2016). TF is a single-chain protein containing 679 amino acid residues with a serum concentration of 2.5 mg mL-1. This protein is divided into two lobes (N and C), each of which contains two domains comprising a series of α-helices and β-sheets. This "multi-task protein" is also involved in growth, differentiation, cytoprotection, and antimicrobial activities apart from its tasks of metal binding and transportation (Chamani, Hanif & Saberi, 2011). TF plays an important role in maintaining the metabolism of iron metabolism and homeostasis (Ding et al., 2015). Several reports on the interaction of TF with different drugs have also been published (Vahedian-Movahed, Saberi & Chamani, 2011). However, the interaction between PGH and TF has not yet been reported. Based on the above reasons, the interaction of the system was studied by spectroscopic method and molecular docking simulation.

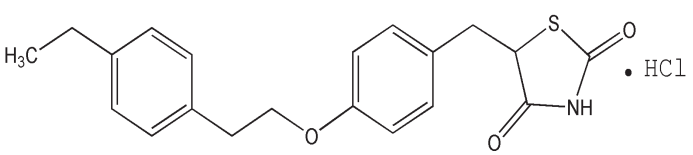

Figure 1. Chemical structure of pioglitazone hydrochloride

2.0 EXPERIMENTAL

2.1 Apparatus and Materials

All fluorescence spectra were recorded with a Shimadzu RF-5301PC spectrofluorophotometer. Absorption was measured with an Ultraviolet-visible recording spectrophotometer (UV-3600, Shimadzu, Japan). Circular dichroism spectra were recorded on a MOS-450/SFM300 circular dichroism spectrometer (Bio-Logic, France). All temperatures were controlled by a CS501 superheated water bath (Nantong Science Instrument Factory).

Bovine transferrin (BTF) was purchased from Sigma Company, Shanghai, China (the purity grade inferior 98.5%). Pioglitazone hydrochloride (the purity grade inferior 98.5%). Stock solutions of BTF (4.0×10^{-6} mol/L) and cefuroxime sodium (1.0×10-3 mol/L) were prepared. All the stock solutions were further diluted as working solutions prior to use. Tris-HCl buffer solution containing NaCl (0.15 mol/L) was used to keep the pH of the solution at 7.4. NaCl solution was used to maintain the ionic strength of the solution. All other reagents were of analytical grade, and all aqueous solutions were prepared with newly double-distilled water and stored at 277 K. The fluorescence data were corrected for absorption of excitation light and emitted light according to the expression given in Equation (1) (Liu, Zhang, Liao & Wang, 2015):

$$F_{\mathrm{c}} = F_{\mathrm{m}} \times e^{(A_1+A_2)/2} \tag{1}$$

where F_c and F_m are the corrected and observed fluorescence intensities, respectively, and A_1 and A_2 are the absorbance values of PGH at excitation and emission wavelengths, respectively. The fluorescence intensity used in this article was corrected.

2.2 Procedures

2.2.1 Ultraviolet-visible Absorption Experiment

At 298 K, 1.0 mL Tris-HCl (pH = 7.40), 1.0 mL BTF solution (4.0×10^{-6} mol/L) and different volume of PGH (1.0×10^{-4} mol/L) were added into 10 mL colorimetric tube successively. The samples were diluted to scaled volume with double-distilled water, mixed thoroughly by shaking, and kept static for 30 min. Ultraviolet-visible absorption spectra of the PGH-BTF system were scanned in the range of 190 nm - 400 nm.

2.2.2 *Fluorescence Measurements*

The fluorescence measurements were carried out as follows: 1.0 mL Tris-HCl (pH = 7.40), BTF solution (4.0×10^{-6} mol/L) and different concentrations of PGH were added into 10 mL colorimetric tube successively. The samples were diluted to scaled volume with double-distilled water, mixed thoroughly by shaking, and kept static for 30 min at different temperatures (298, 310 and 318 K). Excitation wavelength with excitation and emission slit at 5 nm for TBF was 280 nm (or 295 nm), respectively, with a 1.0 cm path length cell. The solution was subsequently scanned on the fluorophotometer and determined the fluorescent intensity.

2.2.3 *Circular Dichroism Spectra Measurements*

The Circular dichroism spectra of BTF in the absence and presence of different amounts of PGH were measured at wavelengths between 190 and 300 nm in pH = 7.4 Tris-HCl buffers under a nitrogen atmosphere at room temperature, and the buffer signal was subtracted. The concentration of BTF was kept at 4.0×10^{-7} mol/L while varying the PGH concentration by keeping the molar ratios of BTF to PGH as 1: 0, 1: 20 and 1: 40.

2.2.4 *Molecular Docking*

The two-dimensional structure of PGH was drawn in ChemDraw 15.0, and its three-dimensional structure was optimized by model of molecular mechanics in ChemDraw3D. The crystal structure of BTF used for molecular docking was obtained from Protein Data Bank (PDB ID: 1d4n). Waters and all other HETATM molecules were removed from the BTF PDB file. Polar hydrogen atoms and Gasteiger charges were added to prepare the BHb molecule for docking. Protein-ligand docking was carried out with the rigid docking tool in the Autodock 4.2.6. In this work, the selection of flexible residues for the induced fit is based on the active site of the BTF. The most favorable docking model was selected according to the binding energy and the geometry matching (Elmas & Esra, 2014).

3.0 RESULTS AND DISCUSSION

3.1 UV-Vis Absorption Studies of PGH-BTF System

The absorption spectra of PGH-BTF combinations are shown in Figure 2. PGH has an absorption maximum at around 200 nm. With increasing concentration of PGH, the intensity of absorption peak at 200 nm decreased with blue shifts. The results suggested that the interaction between PGH and BTF resulted in the formation of a new complex. The intensity of the absorption peak at 275 nm was reduced, illustrating that the interaction between PGH and BTF happened on the ground-state molecules (Li, Liu, Zhang & Han, 2016). Dynamic quenching only affects the excited states of fluorescent molecules and does not alter the absorption spectra of the fluorescent substance (Feng & Yuan, 2009). Therefore, we can infer that the type of fluorescence quenching of BTF by PGH was static quenching.

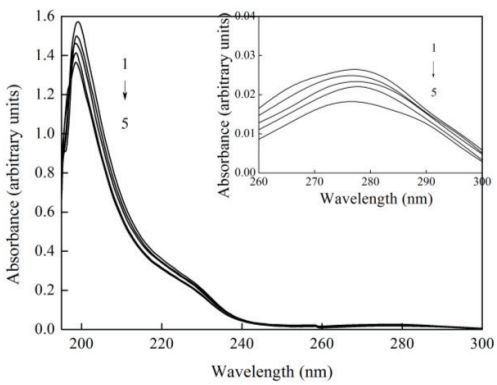

Figure 2. Absorption spectra of PGH-BTF system (T = 298 K)
C_{BTF} = 4.0 × 10^{-7} mol/L, 1~5 C_{PGH} = (0, 2.0, 4.0, 6.0, 8.0) × 10^{-5} mol/L

3.2 Fluorescence Quenching of BTF by PGH

Proteins are considered to have intrinsic fluorescence due to the presence of amino acids, mainly tryptophan and tyrosine. The intrinsic fluorescence of protein is very sensitive to any change of the micro-environment (Shen, Gu, Jian & Qi, 2013). When the excitation wavelength is fixed at 280 nm, tryptophan and tyrosine residues in BTF are excited, whereas at 295 nm, only tryptophan residues are excited (Zhang, Liu, Li & Guo, 2015). When the excitation wavelength was 280 nm (or 295 nm), BTF had a strong fluorescence emission peak at 330 nm. The fluorescence spectra of the BTF-PGH system (λ_{ex} = 280 nm) were shown in Figure 3, demonstrated that the fluorescence intensity of BTF decreased regularly with the addition of PGH when

the excitation wavelength was 280 nm (similar to 295 nm). This result showed that PGH could strongly quench the intrinsic fluorescence of BTF and that there was an interaction between PGH and BTF.

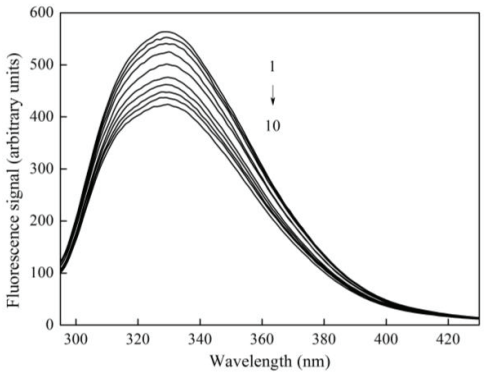

Figure 3. Fluorescence emission spectra of BTF-PGH (T = 298 K)
C_{BTF} = 4.0 × 10^{-7} mol/L, 1~10: C_{PGH} = (0, 1.0, 2.0, 3.0, 4.0, 5.0, 7.0, 8.0, 9.0, 10.0) × 10^{-5} mol/L

In order to confirm the quenching mechanism, the fluorescence quenching data are analyzed by the Stern-Volmer expression, given in Equation (2) (Zhang, Sheng, Zheng & Liu, 2011):

$$F_0 / F = 1 + K_q \tau_0 [Q] = 1 + K_{SV} [Q] \quad (2)$$

where F_0 is the fluorescence intensities in the absence of PGH, F is that in the presence of different concentration of PGH. τ_0 is the average life time of the protein without the quencher (10^{-8} s), and [Q] is the concentration of the quencher. K_{sv} and K_q are the Stern-Volmer quenching constant and the quenching rate constant of biomolecular, respectively. Based on the linear fit plot of F_0/F versus [Q], values of K_{sv} and K_q could be obtained at different temperatures. The calculated results were shown in Table 1. The values of K_{sv} decreased with the rising temperature in all systems, which indicated that the probable quenching mechanism of the interaction between BTF and PGH was initiated by complex formation rather than by dynamic collision (Zhang et al., 2007). In addition, all the values of K_q were much greater than the maximum scatter collision quenching constant of various quenchers (2 × 10^{10} L·mol^{-1} s^{-1}); this also suggested that the quenching was a static process (Wang et al., 2013).

For the static quenching interaction, the binding constants (K_a) and the number of binding sites (n) per molecule can be calculated by the double logarithm expression shown in Equation (3) (Bi, Pang, Wang, Zhao & Yu, 2014):

$$\lg\left(\frac{F_0 - F}{F}\right) = n\lg K_a + \mathrm{n}\lg\left\{\left[D_t\right] - n\frac{F_0 - F}{F}\left[B_t\right]\right\} \quad (3)$$

where F_0 and F are respectively the fluorescence intensities before and after the increase in quencher, $[D_t]$ is the total pigment concentration, and $[B_t]$ is the total protein concentration. The curve of $\log(F_0\text{-}F)/F$ versus $\log\{[D_t]-n(F_0\text{-}F)/F[B_t]\}$ is drawn and linearly fitted, then the value of n can be obtained from the slope of the plot, the value of K_a can be obtained from the value of n and the intercept of the plot. The results were listed in Table 1. From Table 1, we know that the n of BTF and PGH are both about 1 at the λ_{ex} = 280 nm, 295 nm. With the increase of temperature, the K_a of the system decreases, which further explain the static quenching of the interaction system of PGH and BTF (Markarian & Aznauryan, 2012).

Table 1. Quenching reactive parameters of PGH-BTF system at different temperatures

λ_{ex}(nm)	T/(K)	K_q /(L/mol)	K_{sv} /(L/mol)	r_1	K_a /(L/mol)	n	r_2
280	298	6.12×10^{11}	6.12×10^{3}	0.9925	5.46×10^{3}	0.93	0.9982
	310	4.24×10^{11}	4.24×10^{3}	0.9911	4.47×10^{3}	0.97	0.9912
	318	3.33×10^{11}	3.33×10^{3}	0.9900	3.66×10^{3}	0.98	0.9925
295	298	2.92×10^{11}	2.92×10^{3}	0.9956	3.16×10^{3}	1.03	0.9967
	310	2.71×10^{11}	2.71×10^{3}	0.9983	2.82×10^{3}	1.01	0.9998
	318	2.39×10^{11}	2.39×10^{3}	0.9992	2.57×10^{3}	0.95	0.9983

λ_{ex} is the excitation wavelength; K_q is the quenching rate constant; K_{sv} is the Stern-Volmer quenching constant; K_a is the binding constant; n is the number of binding site. r_1 is the linear relative coefficient of F_0/F~$[Q]$; r_2 is the linear relative coefficient of $lg[(F_0\text{-}F)/F]$~$lg\{[D_t]\text{-}n[B_t](F_0\text{-}F)/F_0\}$.

3.3 Type of Interaction Force in PGH-BTF Systems

The intermolecular acting forces between small molecular substrates and biomolecule may be hydrogen bonds, van der Waals interactions, electrostatic interactions, hydrophobic force, etc. (Cao, Liu, Li & Chong, 2014). The thermodynamic parameters of the reaction are important evidence for confirming the binding force. If the temperature varies in a small range, the enthalpy change (ΔH) is regarded as a constant. The values of enthalpy change (ΔH), entropy change (ΔS) and the free-energy change (ΔG) can be evaluated by the van't Hoff plot and thermodynamic given in Equations (4) and (5) (Gong, Zhu, Hu & Yu, 2007):

$$\Delta G = \Delta H - T\Delta S \tag{4}$$

$$R \ln K = \Delta S - \Delta H / T \tag{5}$$

The results are shown in Table 2. If $\Delta H < 0$, $\Delta S > 0$, then the main force between BTF and PGH is electrostatic force. $\Delta G < 0$ indicated that the reaction between them can occur spontaneously (Iovescu et al., 2015).

Table 2. The thermodynamic parameters of BTF-PGH system at different temperatures (λ_{ex} = 280 nm)

T/(K)	K_a/(L·mol^{-1})	ΔH/(KJ·mol^{-1})	ΔS/(J·mol^{-1}·K^{-1})	ΔG/(KJ·mol^{-1})
298	5.46×10^3	-15.48	19.59	-21.32
310	4.47×10^3		19.93	-21.66
318	3.66×10^3		19.53	-21.69

3.4 The Participation of Amino Acid Residues

As seen in Figure 4, in the presence of PGH, the quenching curves of BTF excited at 280 nm and 295 nm overlap below the molar ratio of PGH: BTF = 50: 1. The quenching of BTF fluorescence excited at 280 nm above this molar ratio is slightly higher than that excited at 295 nm. This means that if there are fewer than 50 PGH molecules for 1 BTF molecule, only Trp residue participates in the reaction whereas above this molar ratio both Trp and Tyr residues participate in it.

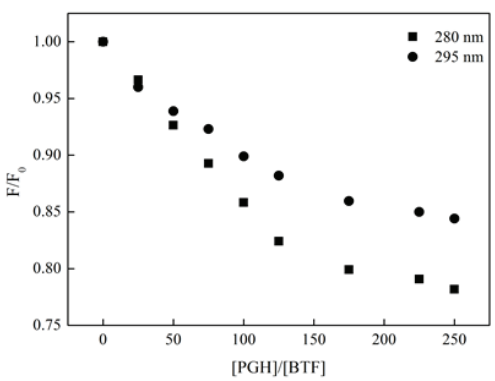

Figure 4. Fluorescence emission spectra of PGH to BTF at λ_{ex} = 280 nm and 295 nm (T = 298 K); C_{BTF} = 4.0 × 10^{-7} mol/L, C_{PGH} = 1.0 × 10^{-5} ~ 1.0 × 10^{-4} mol/L

3.5 PGH Protein Binding Rate

The number of binding sites n = 1, PGH protein binding rate (W) formula is as given in Equations (6) and (7) as follows (Matsui & Okuda, 1988):

$$K_a R[B_0]W^2 - (K_a R[B_0] + K_a[B_0] + 1)W + K_a[B_0] = 0 \quad (6)$$

$$W = \frac{\left(K_a R + K_a + \frac{1}{[B_0]}\right) - \sqrt{\left(K_a R + K_a + \frac{1}{[B_0]}\right)^2 - 4K_a^2 R}}{2K_a R} \quad (7)$$

where R is the ratio of PGH to total protein concentration, $[B_t]$ is the total protein concentration. The protein concentration was 1.0×10^{-3} mol/L, PGH concentration of 1.0×10^{-7}~1.0×10^{-3} mol/L.

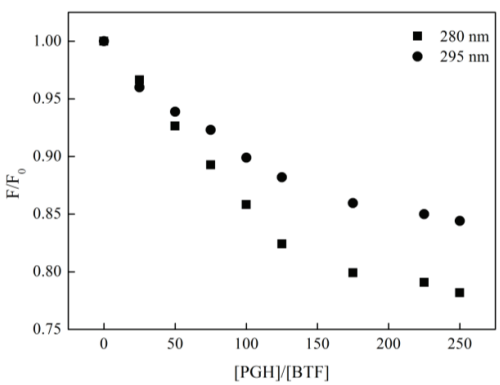

Figure 4. Fluorescence emission spectra of PGH to BTF at λ_{ex} = 280 nm and 295 nm (T = 298 K); C_{BTF} = 4.0 × 10^{-7} mol/L, C_{PGH} = 1.0 × 10^{-5} ~ 1.0 × 10^{-4} mol/L

The experimentally obtained values of K_a and Equation (7) were used to calculate the protein binding rates of different concentrations of PGH at 298, 310 and 318 K with λ_{ex} = 280 nm. Respectively: 65.39%~84.80%, 62.58%~81.72%, 59.63%~78.54%.

As of Figure 5, at 310 K, the nonlinear curve fit equation was: y = -0.06725x^2 - 0.12517x + 0.81733, r = 0.9995, that is W = -0.06725R^2 - 0.12517R + 0.81733. According to above equation, when the concentration of protein in the system is constant, the protein binding rate decreased with the addition of PGH. The protein binding rate of PGH provides important reference value for clinical medicine.

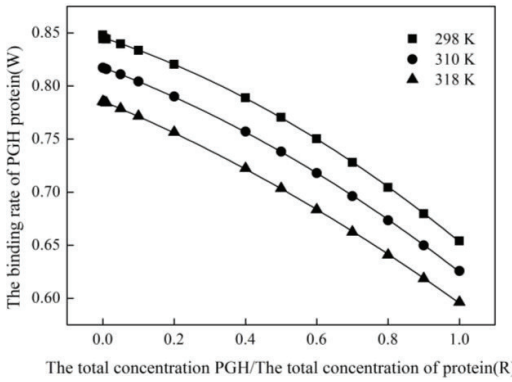

Figure 5. The binding rate of PGH to protein in different temperature (λ_{ex} = 280 nm)

3.6 Binding Distances Between PGH and BTF

According to Förster's non-radiative energy transfer theory, energy efficiency E, critical energy-transfer distance R0 (E = 50%), the energy donor and the energy acceptor distance r and the overlap integral between the fluorescence emission spectrum of the donor and the absorption spectrum of the acceptor J can be calculated by the formula shown in Equations (8) to (10) as follows (Fabini, Fiori, Tedesco, Lopes & Bertucci, 2016; Zhao, Liu & Teng, 2011):

$$E = 1 - F / F_0 = R_0^{\ 6} / (R_0^{\ 6} + r^6) \quad (8)$$

$$R_0^{\ 6} = 8.79 \times 10^{-25} K^2 \Phi N^{-4} J \quad (9)$$

$$J = \sum F(\lambda)\varepsilon(\lambda)\lambda^4 \Delta\lambda / \sum F(\lambda)\Delta\lambda \quad (10)$$

where K^2 is the orientation factor, Φ is the fluorescence quantum yield of the donor, N is the refractive index of the medium, $F(\lambda)$ is the fluorescence intensity of the fluorescence donor at wavelength λ and $\varepsilon(\lambda)$ is the molar absorption coefficient of the acceptor at this wavelength. The overlap of UV-vis absorption spectra of PGH and the fluorescence emission spectra of BTF (λ_{ex} = 280 nm) are shown in Figure 6. Under these experimental conditions, it has been reported that K2 = 2/3, N = 1.336 and Φ = 0.118. Thus J, E, R_0 and r were calculated and shown in Table 3. The donor-to-acceptor distance $r < 7$ nm indicated that the energy transfers from BTF to PGH occurred with high possibility. Further the value of r was greater than R_0 in this study which suggested that PGH

could strongly quench the intrinsic fluorescence of BTF by a static quenching mechanism (Buddanavar & Nandibewoor, 2017). Moreover, the distance *r* increased and the energy efficiency *E* decreased with increasing temperature, which resulted in the reduced stability of the binary systems and the values of K_a.

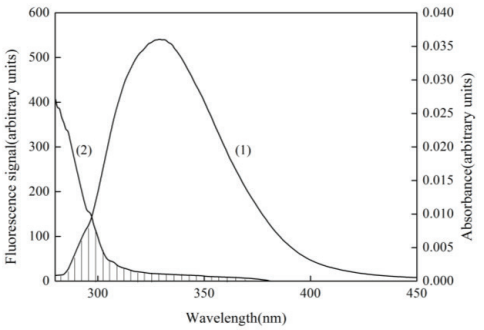

Figure 6. Fluorescence emission spectra (λex = 280 nm) (1) for BTF and UV absorbance spectra for PGH (2) (T = 298 K); CBTF = CPGH = 4.0 × 10-7 mol/L

Table 3. Parameters of E, J, r, R0 between PGH and BTF at different temperatures

***T*/(K)**	***E*/(%)**	***J*/(cm^3·L/mo**	***R_0*/(nm)**	***r*/(nm)**
298	4.01	6.93×10^{-15}	2.16	3.60
310	3.88	6.08×10^{-15}	2.11	3.66
318	3.17	5.90×10^{-15}	2.10	3.71

3.7 Circular Dichroism Measurements

Circular dichroism (CD) can be used to display protein conformation changes. The diagram of the CD combined with PGH-BTF is shown in Figure 7. There is a characteristic peak of α-helix near 211 nm. When the C_{BTF}: *CPGH* was 1: 20 and 1: 40, the height of the negative peak decreases, and the position and shape of the peak did not change. The results showed that α-helix loosened and the fluorescence quenching of BTF and the existence of PGH changed the conformation of BTF, but α-helix was still the main structural form of BTF (Yuan et al., 2017).

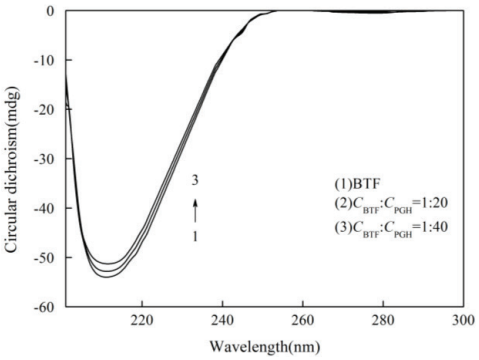

Figure 7. The circular dichroism spectra of PGH-BTF system (T = 298 K)
C_{BTF} = 4.0 × 10^{-7} mol/L; C_{PGH} = (2, 4) × 10^{-5} mol/L

3.8 Molecular Docking

To further illustrate the interaction mechanism of PGH and BTF, we use molecular simulation technology to further explore this process. The molecular docking results showed that the binding energy of PGH and BTF ΔG is -21.32 kJ/mol. This result and the experimental results (-22.17 kJ/mol) are the same, showing that this binding mode can truly reflect the reaction between PGH and BTF. The optimum binding mode and site was displayed in Figure 8, and the amino acid residues surrounding PGH were captured. PGH was surrounded by amino acid residues of LEU46, TYR45, ASP69, LEU72, GLY123, LEU122, ARG327, LEU328, TRP128, PRO145, LEU14, LYS144 and ARG143, most of which are hydrophobic amino acid residues. The results showed that the interaction between PGH and BTF was driven mainly by hydrophobic interaction, and PGH can effectively make the fluorescence quenching of BTF, which was consistent with the experimental results of fluorescence spectrum (Raza et al., 2017).

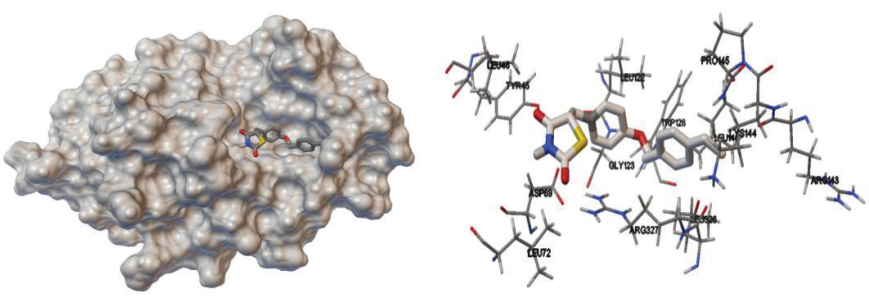

Figure 8. Computation docking model of the interaction between PGH and BTF. (A)Binding site in the BTF cavity. (B) Detailed illustration of the amino acid residues lining the binding site in the BTF cavity.

4.0 CONCLUSION

The reaction mechanism between PGH and BTF was studied in detail by means of spectral method and molecular docking simulation technique. The results showed that the fluorescence quenching of BTF is due to the formation of PGH-BTF complex, which was accompanied by non-radiative energy transfer. CD spectra showed that the secondary structure of BTF microenvironment changed with the addition of PGH. The thermodynamic parameters were obtained by thermodynamic equation and the results agreed with the molecular docking technique. It was further shown that the binding mode of PGH and BTF is mainly electrostatic gravity. At the same time, the experimental results are of great help to understand the substance of drug efficacy and provide a more meaningful theoretical basis for the research and development of drugs.

ACKNOWLEDGMENTS

The authors gratefully acknowledge the financial support of National Natural Science Foundation of China (No. 21375032).

REFERENCES

Bi, S. Y., Pang, B., Wang, T. J., Zhao, T. T., Yu, W. (2014). Investigation on the interactions of clenbuterol to bovine serum albumin and lysozyme by molecular fluorescence technique. *Spectrochimica Acta Part A-Molecular and Biomolecular Spectroscopy*, 120(4):456-461.

Bai, L. N., Qiao, M., Zheng, R., Deng, C. Y., Mei, S. Q., Chen, W. P. (2016). Phylogenomic analysis of transferrin family from animals and plants. *Comparative Biochemistry and Physiology D-genomics & Proteomics*, 17(1):1-8.

Buddanavar, A. T., Nandibewoor, S. T. (2017). Multi-spectroscopic characterization of bovine serum albumin upon interaction with atomoxetine. *Journal of Pharmaceutical Analysis*, 7:148-155.

Chamani, J. K., Hanif, V. M., Saberi, M. R. (2011). Lomefloxacin promotes the interaction between human serum albumin and transferrin: A mechanistic insight into the emergence of antibiotic's side effects. *Journal of Pharmaceutical and Biomedical Analysis*, 55(1):114-124.

Cao, S. N., Liu, B. S., Li, Z. Y., Chong, B. H. (2014). A fluorescence spectroscopic study of the interaction between Glipizide and bovine serum albumin and its analytical application. *Journal of Luminescence*, 145:94-99.

Ding, Z. J., Zhao, X. H., Su, L. N., Zhou, F. J., Chen, N., Wu, J. J., Fu, X. Q., Wu, F., Wang, W. F., Liu, H. (2015). The Megalobrama amblycephala transferrin and transferrin receptor genes: Molecular cloning, characterization and expression during early development and after Aeromonas hydrophila infection. *Developmental and Comparative Immunology*, 49(2):290-297.

Elmas, G., Esra, Y. (2014). Fluorescence interaction and determination of sulfathiazole with trypsin. *Journal of Fluorescence*, 24:1439-1445.

Feng, S. L., Yuan, D. Q. (2009). Study on interaction between piperazine ferulate and bovine serum albumin. *Journal of Clinical Laboratory Analysis*, 28:78-82.

Fabini, E., Fiori, G. M. L., Tedesco, D., Lopes, N. P., Bertucci, C. (2016). Surface plasmon resonance and circular dichroism characterization of cucurbitacins binding to serum albumins for early pharmacokinetic profiling. *Journal of Pharmaceutical and Biomedical Analysis*, 122:166-172.

Gong, A. Q., Zhu, X. S., Hu, Y. Y., Yu, S. H. (2007). A fluorescence spectroscopic study of the interaction between epristeride and bovin serum albumine and its analytical application. *Talanta*, 73:668-673.

Iovescu, A., Baran, A., Stinga, G., Cantemir-Leonties, A. R., Maxim, M. E., Anghel, D. F. (2015). A combined binding mechanism of nonionic ethoxylated surfactants to bovine serum albumin revealed by fluorescence and circular dichroism. Journal of Photochemistry and Photobiology B-biology, 153:198-205.

Lin, J. J., Liu, Y., Chen, M. M., Huang, H. Y., Song, L. (2014). Investigation on the binding activities of citalopram with human and bovine serum albumins. *Journal of Luminescence*, 146:114-122.

Liu, Y. Y., Zhang, G. W., Liao, Y. J., Wang, Y. P. (2015). Binding characteristics of psoralen with trypsin: Insights from spectroscopic and molecular modeling studies. *Spectrochimica Acta Part A: Molecular and Biomolecular Spectroscopy*, 151:498-505.

Li, G. X., Liu, B. S., Zhang, Q. J., Han, R. (2016). Investigation on the effect of fluorescence quenching of bovine serum albumin by cefoxitin sodium using fluorescence spectroscopy and synchronous fluorescence spectroscopy. *Luminescence*, 31:1054-1062.

Matsui, H., Okuda, T. (1988). Penetration of cefpiramide and cefazolin into peritoneal capsular fluid in rabbits. *Antimicrobial Agents and Chemotherapy*, 32(1):33-36.

Markarian, S. A., Aznauryan, M. G. (2012). Study on the interaction between isoniazid and bovine serum albumin by fluorescence spectroscopy: The effect of dimethylsulfoxide. *Molecular Biology Reports,* 39(7):7559-7567.

Raza, M., Yang, J., Yun, W., Ahmad, A., Khan, A., Yuan, Q. P. (2017). Insights from spectroscopic and in-silico techniques for the exploitation of biomolecular interactions between Human serum albumin and Paromomycin. *Colloids and Surfaces B: Biointerfaces*, 157:242-253.

Shen, H. B., Gu, Z. Q., Jian, K., Qi, J. (2013). In vitro study on the binding of gemcitabine to bovine serum albumin. *Journal of Pharmaceutical and Biomedical Analysis*, 75:86-93.

Takagi, T., Ramachandran, C., Bermejo, M., Yamashita, S., Yu, L. X., Amidon, G. L. (2006). A provisional biopharmaceutical classification of the top 200 oral drug products in the United States, Great Britain, Spain, and Japan. *Molecular Pharmaceutics*, 3(6):631-643.

Vahedian-Movahed, H., Saberi, M. R., Chamani, J. (2011). Comparison of binding interaction of lomefloxacin to serum albumin and serum transferrin by resonance Rayleigh scattering and fluorescence quenchingmethods. *Journal of Biomolecular Structure & Dynamics*, 28:483-502.

Wang, R. Y., Kang, X. H., Wang, R. Q., Wang, R., Dou, H. J., Wu, J., Song, C. J., Chang, J. B. (2013). Comparative study of the binding of trypsin to caffeine and theophylline by spectrofluorimetry. *Journal of Luminescence*, 138:258-266.

Yuan, L. X., Liu, M., Sun, B., Liu, J., Wei, X. L., Wang, Z. P., Wang, B. Q., Han, J. (2017). Calorimetric and spectroscopic studies on the competitive behavior between (−)-epigallocatechin-3-gallate and 5-fluorouracil with human serum albumin. *Journal of Molecular Liquids*, 248:330-339.

Zhang, G. J., Keita, B. J., Brochon, C., Pedrode, O., Nadjo, L., Craescu, C. T., Miron, S. (2007). Molecular interaction and energy transfer between human serum albumin and polyoxometalates. *Journal of Physical Chemistry B*, 111(7):1809-1814.

Zhang, X. C., Sheng, F., Zheng, J. L., Liu, R. T. (2011). Composition and stability of anthocyanins from purple solanum tuberosumand their protective influenceon Cr(VI) targetedto bovine serum albumin. *Journal of Agricultural and Food Chemistry*, 59:7902-7909.

Zhao, X. C., Liu, R. T., Teng, Y. (2011). The interaction between Ag+ and bovine serum albmin: a spectroscopic investigation. *Sci Total Environ*, 409(5):892-897.

Zhang, L. H., Liu, B. S., Li, Z. Y., Guo, Y. (2015). Comparative Studies on the Interaction of Aspirin with Bovine Serum Albumin by Fluorescence Quenching Spectroscopy and Synchronous Fluorescence Spectroscopy. *Spectroscopy Letters*, 48(6):441-446.

Zhang, C. C., Matzger, A. J. (2017). A Newly Discovered Racemic Compound of Pioglitazone Hydrochloride Is More Stable than the Commercial Conglomerate. *Crystal Growth & Design*, 17(2):414-417.